

1 **Complex roles for proliferating cell nuclear antigen in restricting human cytomegalovirus**
2 **replication**

3
4 Pierce Longmire^{1,2,3}, Olivia Daigle^{4,5}, Sebastian Zeltzer³, Matias Lee⁵, Marek Svoboda⁴, Marco
5 Padilla-Rodriguez⁶, Carly Bobak⁵, Giovanni Bosco⁴, and Felicia Goodrum^{1,2,3}#
6

7 ¹Graduate Program in Molecular Medicine, University of Arizona, Tucson, Arizona, USA

8
9 ²Department of Immunobiology, University of Arizona, Tucson, Arizona, USA

10
11 ³BIO5 Institute, University of Arizona, Tucson, Arizona, USA

12
13 ⁴Department of Molecular and Systems Biology, Dartmouth Geisel College of Medicine,
14 Hanover, New Hampshire, USA

15
16 ⁵Research Computing and Data Services, Information, Technology, and Consulting, Dartmouth
17 College, Hanover, New Hampshire, USA

18
19 ⁶Microscopy Shared Resource, University of Arizona Cancer Center, Tucson, Arizona, USA

20
21 Running title: PCNA restricts HCMV replication

22
23 #Address correspondence to Felicia Goodrum, fgoodrum@arizona.edu
24

25 **ABSTRACT**

26 DNA viruses at once elicit and commandeer host pathways, including DNA repair pathways for
27 virus replication. Despite encoding its own DNA polymerase and processivity factor, human
28 cytomegalovirus (HCMV) recruits the cellular processivity factor, proliferating cell nuclear
29 antigen (PCNA) and specialized host DNA polymerases involved in translesion synthesis (TLS)
30 to replication compartments (RCs) where viral DNA (vDNA) is synthesized. While the
31 recruitment of TLS polymerases is important for viral genome stability, the role of PCNA is
32 poorly understood. PCNA function in DNA repair is regulated by monoubiquitination (mUb) or
33 SUMOylation of PCNA at lysine 164 (K164). We find that mUb-PCNA increases over the course
34 of infection, and modification of K164 is required for PCNA-mediated restriction of virus
35 replication. mUb-PCNA plays important known roles in recruiting TLS polymerases to DNA,
36 which we have shown are important for viral genome integrity and diversity, represented by
37 novel junctions and single nucleotide variants (SNVs), respectively. We find that PCNA drives
38 SNVs on vDNA similar to Y-family TLS polymerases, but that this did not require modification at
39 K164. Unlike TLS polymerases, PCNA was dispensable for preventing large scale
40 rearrangements on vDNA. These striking results suggest separable PCNA-dependent and -
41 independent functions of TLS polymerases on vDNA. By extension, these results imply roles for
42 TLS polymerase beyond their canonical function in TLS in host biology. These findings highlight
43 PCNA as a complex restriction factor for HCMV infection, likely with multiple distinct roles, and
44 provides new insights into the PCNA-mediated regulation of DNA synthesis and repair in viral
45 infection.

46

47

48 **IMPORTANCE**

49 Genome synthesis is a critical step of virus life cycles and a major target of antiviral drugs.

50 Human cytomegalovirus, like other herpesviruses, encodes machinery sufficient for viral DNA

51 synthesis and relies on host factors for efficient replication. We have shown that host DNA repair

52 factors play important roles in HCMV replication, but our understanding of this is incomplete.

53 Building on previous findings that specialized host DNA polymerases contribute to HCMV

54 genome integrity and diversity, we sought to determine the importance of PCNA, the central

55 polymerase regulator. PCNA associates with nascent viral DNA and restricts HCMV replication.

56 While PCNA is dispensable for genome integrity, it contributes to genome diversity. Our findings

57 suggest that host polymerases function on viral genomes by separable PCNA-dependent and -

58 independent mechanisms. Through revealing complex roles for PCNA in HCMV replication, this

59 study expands the repertoire of host DNA synthesis and repair proteins hijacked by this

60 ubiquitous herpesvirus.

61

62

63 INTRODUCTION

64 Human cytomegalovirus (HCMV) is a ubiquitous herpesvirus that has co-evolved with
65 humans and persists in a majority of the world's population through establishment of latent
66 infection. Latency is defined as a quiescent infection where viral genomes are maintained in the
67 absence of viral genome synthesis and viral progeny production (1). For HCMV, progenitor cells
68 of the myeloid lineage and monocytes have been described as a major reservoir for latency (2,
69 3). While most seropositive individuals experience asymptomatic infection, HCMV reactivation
70 from latency poses serious disease and mortality risk for immunocompromised individuals
71 including solid organ and stem cell transplant recipients. Infection during pregnancy and viral
72 transmission to the fetus occurs in 1 in 200 births in the United States. Of these newborns with
73 congenital infection, 20% will develop permanent disabilities, making HCMV the leading cause
74 of infectious disease-related birth defects in the United States (4, 5). There are no clinical
75 strategies to target or control latent HCMV infection due to limited knowledge of how the virus
76 toggles between latent and replicative states. Complex interplay between viral determinants and
77 host biology is central to regulation of viral gene expression, genome amplification, and decision
78 to establish latency or replicate (6). Consequently, investigating these virus-host interactions at
79 a molecular level is important to building a mechanistic understanding of latency and
80 reactivation.

81 While HCMV encodes several proteins sufficient for viral DNA (vDNA) synthesis, it also
82 relies on its host for specific factors that may fine-tune or modulate specific aspects of
83 synthesis. HCMV infection drastically alters cell cycle progression (7) and induces E2F1
84 transcription factor activity, which regulates many host DNA synthesis and repair genes (8).
85 Virus replication also activates DNA damage response signaling through major kinases, ataxia-
86 telangiectasia mutated (ATM) and ataxia-telangiectasia Rad3-related (ATR) (9). Many of the
87 downstream repair proteins are re-localized to nuclear viral replication compartments (RCs),
88 sites of vDNA synthesis, but their specific contributions to the viral replication cycle are poorly

89 understood (8-11). In previous studies, we found that HCMV recruits specialized host DNA
90 polymerases involved in translesion synthesis (TLS) pathways to modulate virus replication
91 despite encoding its own DNA polymerase, *UL54*. TLS is a DNA damage bypass pathway in
92 which specialized polymerases are recruited to replication forks or sites of damage in order to
93 synthesize through lesions and prevent replication fork stalling or collapse (12). TLS
94 polymerases lack proofreading activity and have a warped active site compared to replicative
95 DNA polymerases, which allows for synthesis across DNA lesions albeit with lower fidelity (13).
96 Therefore, TLS is a double-edged sword in which bulky nucleotide lesions may be bypassed
97 during replication in a process that comes at the cost of potentially introducing small point
98 mutations into newly synthesized DNA. We specifically found that the Y-family polymerases eta
99 (η), kappa (κ), and iota (ι) restrict vDNA synthesis and viral replication, while the B-family
100 polymerase zeta (ζ) and its putative scaffold, Y family polymerase Rev1, are required for
101 efficient vDNA synthesis and virus replication. Despite these polymerases having opposite
102 effects on viral replication, all are required for viral genome integrity whereby the depletion of
103 either group of polymerases results in a significant increase in aberrant recombination and novel
104 DNA junctions, primarily inversions, across the viral genome (14).

105 Proliferating cell nuclear antigen (PCNA) is an essential sliding clamp that acts as a
106 processivity factor, maintaining polymerase association with DNA and promoting processivity of
107 DNA synthesis (15). Normally, PCNA interacts with B-family DNA polymerases delta (δ) and
108 epsilon (ϵ) through a PCNA interacting protein (PIP) motif (15). At sites of damage, PCNA is
109 monoubiquitinated (mUb-PCNA) at lysine residue 164 (K164) by the E3 ubiquitin ligase, RAD18,
110 to promote its association with TLS polymerases and subsequent damage bypass (16). TLS
111 polymerase have less well-defined function in other DNA repair pathways that occur
112 independently of PCNA (17-20). HCMV also encodes a viral DNA polymerase processivity
113 factor, *UL44*, which is essential for virus replication (21). Like PCNA, pUL44 is a processivity

114 factor that interacts with pUL54 to maintain polymerase-DNA interactions. Comparing the two,
115 both PCNA and pUL44 are sliding clamps that associate with DNA, but they share no sequence
116 similarity (22). Additionally, PCNA is a homotrimer that undergoes extensive post-translational
117 modifications to regulate interacting partners (23). By contrast, pUL44 is a homodimer with few
118 characterized post-translational modifications and viral interacting partners (24-26). Despite
119 these differences, pUL44 and pUL54 are thought to function similarly to PCNA and replicative
120 cellular B-family polymerases as a clamp-polymerase complex to facilitate vDNA synthesis (21,
121 27). We sought to better understand the role of PCNA in HCMV replication.

122 We previously observed that HCMV infection in fibroblasts induces monoubiquitination of
123 PCNA and, in line with observations from others, re-localization of PCNA to viral RCs (14, 28-
124 30). This observation was consistent with the roles we found for TLS polymerases in regulating
125 HCMV genome integrity and replication. However, the significance of PCNA to HCMV genome
126 synthesis, integrity, and replication remains to be defined. Here, we found that PCNA restricted
127 viral replication in the TB40/E strain in a manner that was dependent on PCNA and its
128 modification at the K164 residue. Homing in on this monoubiquitination, we found that
129 accumulation of mUb-PCNA depended on viral DNA synthesis. Further, PCNA and mUb-PCNA
130 localized to distinct subdomains in RCs relative to replication forks and viral proteins important
131 for vDNA synthesis. However, unlike the TLS polymerases that mUb-PCNA would presumably
132 recruit, PCNA and mUb-PCNA were not required for protecting the vDNA from large
133 rearrangements. Instead, we found that PCNA contributed to genome diversity through
134 generating SNVs on viral DNA, similar to Y-family TLS polymerases. These results suggest that,
135 while the SNVs generated on viral DNA by TLS polymerases are PCNA-dependent, TLS
136 polymerase-moderated genome stability occurs independently of PCNA. Altogether this work
137 uncovers specific contributions of PCNA to HCMV infection and highlights the complexity of this
138 virus-host interaction.

139

140 **RESULTS**

141 **mUb-PCNA increases with viral DNA synthesis**

142 Given the role of TLS polymerases to HCMV infection and their dependence on mUb-
143 PCNA in host cells, we sought to build on our findings by further characterizing mUb-PCNA in
144 the context of HCMV infection. To better define the relationships between PCNA, mUb-PCNA,
145 and vDNA synthesis, we inhibited viral DNA synthesis with phosphonoacetic acid (PAA) and
146 analyzed the accumulation of PCNA and mUb-PCNA. PAA is a small molecule that binds the
147 viral polymerase, pUL54, and blocks the pyrophosphate binding site, ultimately inhibiting
148 polymerase activity (31, 32). Cells were treated with PAA at the onset of infection (TB40/E-WT
149 or mock). In mock-infected cells mUb-PCNA decreased as cells grew to confluence, and PAA
150 treatment had no effect on this over the 96 hours post infection (hpi) time course (Fig. 1A,
151 quantified in 1B). HCMV-infected cells accumulated mUb-PCNA as infection progressed,
152 consistent with previous findings (14), while levels did not change in PAA-treated cells (Fig 1A,
153 quantified in 1C). Further, unlike mock-infected cells, HCMV infection maintained mUb-PCNA
154 despite increasing cell confluence. These data suggest that HCMV vDNA synthesis drives
155 accumulation of mUb-PCNA.

156

157 **PCNA restricts HCMV TB40/E replication**

158 Given that mUb-PCNA is associated with viral DNA synthesis, we hypothesized that
159 PCNA is functionally important for viral replication. We stably disrupted PCNA expression via
160 shRNA depletion under growth arrest conditions in order to avoid replication stress and cell
161 death due to depletion of this essential host factor. Compared to cells expressing shRNA
162 against firefly Luciferase (Luc, non-targeting control), we achieved ~70% knockdown of PCNA
163 protein over multiple independent experiments (Fig. 2A). Compared to the Luc control, depletion
164 of PCNA resulted in a ~2 log increase in virus yield, suggesting that PCNA restricts HCMV
165 replication (Fig. 2B). Consistent with this, we also measured viral genome copy number at 15

166 days post infection and observed an increase with depletion of PCNA (Fig. 2C). Cells depleted
167 of PCNA infected at a multiplicity of infection (MOI) of 1 and collected over a 96-hour time
168 course exhibited a 4-fold increase in viral titers (Fig. 2D), but no significant increase in viral
169 genomes (Fig. 2E). Therefore, PCNA restricts HCMV replication and genome synthesis, and the
170 PCNA-mediated restriction of viral genome synthesis and progeny production was less apparent
171 at higher MOIs of infection but not fully overcome.

172 To understand how PCNA affects viral gene expression, we further analyzed the impact
173 of PCNA on viral gene expression (Fig. 2F). Comparing between Luc and PCNA knockdown, we
174 observed no differences in immediate early proteins (IE1/2) or a representative early protein,
175 pUL44. Protein levels of IE1/2 and pUL44 from three independent experiments are quantified in
176 Figures 2G and 2H, respectively. Therefore, PCNA does not impact viral gene expression early
177 during infection. However, the late protein, pp150 was increased at 72 hours post infection (hpi),
178 although increases in another late protein, pp28, did not reach statistical significance relative to
179 the Luc control (Fig. 2I-J). Taken together, these data suggest that the restriction imposed by
180 PCNA on vDNA synthesis is reflected in reduced viral gene expression late in infection.

181 Our observation that PCNA restricts HCMV replication is surprising considering that
182 PCNA is re-localized to HCMV RCs and supports viral DNA synthesis for other herpesviruses
183 (33-35). Specifically, PCNA is required for replication of the alpha-herpesvirus, herpes simplex
184 virus 1 (HSV-1) (35, 36), a finding that we recapitulate when we infect PCNA-depleted cells with
185 HSV-1 (Fig. 2K). Further, PCNA depletion has been shown to decrease genome synthesis in the
186 lab adapted AD169 strain of HCMV (30), which we also observe when measuring virus yield
187 (Fig. 2L). These results suggest that the restriction imposed by PCNA on HCMV replication is
188 due to genes or attributes specific to low-passage strains of HCMV.

189

190 **K164 modification on PCNA mediates restriction of HCMV TB40/E replication**

191 To build upon our finding that PCNA restricts HCMV TB40/E replication, we sought to
192 determine the significance of mUb-PCNA during infection. In response to DNA damage, PCNA
193 is monoubiquitinated on lysine 164 (K164) by the E3 ubiquitin ligase, RAD18, facilitating
194 interactions with TLS polymerases (37, 38). PCNA is also modified on K164 by
195 polyubiquitination to activate an alternate, error-free DNA lesion bypass through a post-
196 replicative, template-switching mechanism (37, 39, 40). Further, K164 may also be modified by
197 small ubiquitin-like modification (SUMOylation) to antagonize homologous recombination DNA
198 repair (41, 42). In order to investigate the significance of post-translational modifications on the
199 K164 residue, we generated two shRNA-resistant PCNA constructs through wobble codon
200 mutagenesis: wild-type PCNA and a mutant in which K164 is mutated to arginine (K164R),
201 preventing both ubiquitination and SUMOylation on this residue.

202 To determine how K164 modification on PCNA impacts HCMV replication, we generated
203 lentivirus particles to deliver these constructs alongside shRNA in an attempt to rescue
204 phenotypes associated with PCNA depletion. While overexpression of wild-type PCNA resulted
205 in monoubiquitination of PCNA, expression of the K164 variant of PCNA resulted in minimal
206 detection of mUb-PCNA as expected (Fig. 3A). Cells expressing these constructs were infected
207 at an MOI of 1 and collected at 96 hpi. For controls, we also compared cells expressing shRNA
208 against Luc or PCNA with no rescue (Empty).

209 As expected, PCNA knockdown with empty rescue recapitulated a ~five-fold increase in
210 virus yield over Luc control conditions. In comparison, PCNA knockdown with wild-type PCNA
211 expression yielded no significant change in virus replication compared to Luc, demonstrating a
212 partial phenotypic rescue (Fig. 3B). PCNA-K164R rescue resulted in replication at levels similar
213 to PCNA depletion alone, suggesting that PCNA-mediated restriction of HCMV replication
214 depends on modification of K164. Despite the effect on virus replication, PCNA K164R did not
215 impact viral genome copy number (Fig. 3C), similar to our results with PCNA knockdown at this
216 MOI (Fig. 2E). Therefore, PCNA restricts HCMV replication in a manner dependent on

217 modification at the K164 residue, although we cannot differentiate the importance of
218 ubiquitination or SUMOylation of this residue.

219

220 **mUb-PCNA localizes to distinct replication compartment subdomains**

221 PCNA localizes to viral replication compartments (14, 28-30), suggesting a role for
222 PCNA in vDNA synthesis. However, the virus encodes its own functional homologue of PCNA,
223 pUL44, that is important for processivity of the viral DNA polymerase, pUL54 (21, 43, 44). To
224 better understand the interplay between pUL44 and either PCNA or mUb-PCNA, we analyzed
225 their localization in viral RCs and colocalization to replication forks. Active sites of vDNA
226 synthesis labeled with EdU have been localized to the periphery of RCs with pUL44 in HCMV
227 infection (45), suggesting that viral DNA synthesis occurs at the periphery. However, others
228 have observed active DNA synthesis throughout HCMV and HSV-1 RCs using either 5-ethynyl-
229 2'-deoxyuridine (EdU) or 5-ethynyl-2'-deoxycytidine (EdC) nucleotide analogs (36, 46, 47). We
230 used this technique to analyze the association of PCNA and mUb-PCNA with sites of active
231 synthesis of vDNA relative to pUL44 or the HCMV single-stranded DNA binding protein, pUL57,
232 which also localizes to RCs (48). To ensure labeling only of viral RCs, fibroblasts were growth
233 arrested prior to infection and maintained in serum-free conditions. At 48 hpi, we pulsed cells
234 with EdU for 10 min and localized PCNA, mUb-PCNA, pUL44, and pUL57 by indirect
235 immunofluorescence to assess their association with EdU-labeled replication forks.

236 EdU labeling was specifically incorporated throughout the RCs of infected cells (Fig. 4).
237 PCNA exhibited stronger colocalization with EdU than either pUL44 (Fig. 4A) or pUL57 (Fig.
238 4B). However, mUb-PCNA was more distantly associated with EdU than pUL44 (Fig. 4C) or
239 pUL57 (Fig. 4D), suggesting a possible role post-synthesis. Because we did not observe EdU
240 incorporation at the periphery of RCs as previously reported by Strang et al. (45), we analyzed
241 EdU labeling in cells infected with the AD169 laboratory-adapted strain in case virus strain
242 accounted for these differences. EdU was incorporated throughout the RCs similarly to TB40/E

243 infection (Fig. S1). The differences between the observations reported here and those by Strang
244 et al. may be due to cell type or MOI differences. However, incorporation of EdU throughout
245 RCs has been reported by others in HCMV and HSV-1 infection (36, 46, 47).

246

247

248 **PCNA contributes to HCMV genome diversity but not integrity**

249 Our findings thus far point to a role for PCNA in regulating HCMV genome synthesis and
250 replication. As an essential factor for eukaryotic DNA replication and repair, we wondered the
251 extent to which PCNA influences viral genome integrity. In previous studies, we found that TLS
252 polymerases are required for HCMV genome integrity (14). While TLS polymerases can function
253 in DNA repair independently of PCNA (17, 19, 20), PCNA and its mUb is critical to recruit TLS
254 polymerases to lesions for canonical translesion synthesis (15, 23). Building on findings
255 presented here, we sought to determine if depletion of PCNA alone was sufficient to
256 compromise viral genome integrity in HCMV TB40/E infection and if genome integrity depended
257 on modification at K164R. To assess this, we sequenced genomic DNA extracted from HCMV-
258 infected fibroblasts expressing shRNAs against Luciferase or PCNA with expression of an
259 empty vector or PCNA K164R as described (Fig. 3A) and quantitated novel DNA junctions
260 (inversions, duplications, and deletions) and single nucleotide variations (SNVs; point mutations,
261 small deletions, and insertions) arising in synthesized viral genomes compared to the parental
262 virus stock used for infection. Strikingly, we found that neither depletion of PCNA nor rescue
263 with the K164R mutant significantly impacted large genomic rearrangements compared to the
264 Luc control (Fig. 5A, quantified in 5B). This was a surprising result given the role for PCNA in
265 recruiting TLS polymerases. By contrast, depletion of TLS polymerases, increased inversions,
266 duplication and deletions across the viral genome (14). However, similar to depletion of TLS
267 polymerases (14), depletion of PCNA resulted in fewer SNVs on the viral genome, but SNVs are
268 generated independently of modification at K164R (Fig. 5C). Taken together, these results

269 suggest that PCNA is dispensable in the maintenance of HCMV genome integrity but could
270 drive genome diversity.

271

272

273 **DISCUSSION**

274 As intracellular parasites, all viruses rely on host cell factors for efficient replication. Even
275 complex DNA viruses, like herpesviruses, hijack their host's machinery despite encoding similar
276 factors of their own. Our current knowledge of the involvement of host factors in the HCMV
277 replicative program, especially at the step of vDNA synthesis, is incomplete. Building on our
278 previous findings that TLS polymerases are recruited to viral RCs and modulate HCMV
279 replication and genome integrity (14), we set out to define roles of the host DNA processivity
280 factor and polymerase binding partner, PCNA, in HCMV replication. While PCNA is best known
281 for its role in increasing polymerase processivity, it also plays important role in DNA repair (15).
282 Post-translational modifications, such as ubiquitination or SUMOylation, direct its engagement
283 with repair processes. We show that HCMV infection induces monoubiquitination of PCNA, a
284 modification important for recruiting TLS polymerases. PCNA activity on vDNA restricts vDNA
285 synthesis and HCMV replication and post-translational modifications (i.e., monoubiquitination or
286 SUMOylation) at the K164 residue are important for this restriction (Fig. 3B). Despite having a
287 role in viral DNA synthesis, PCNA depletion did not affect viral genome integrity (Fig. 5 A and B),
288 as depletion of TLS polymerases does (14). However, PCNA was required for generating SNVs
289 on viral DNA, similar to Y-family TLS polymerases, η , κ , and ι (Fig. 5C), suggesting that TLS
290 polymerases function on the viral genome by both PCNA-dependent and -independent
291 mechanisms. Additionally, unmodified PCNA and mUb-PCNA were differentially associated with
292 sites of active vDNA synthesis (Fig. 4), further emphasizing the multifaceted role of PCNA in
293 regulating HCMV replication. This work highlights PCNA as a restriction factor to HCMV
294 replication with complex roles that remain to be defined.

295 With no enzymatic activity, PCNA undergoes multiple post-translational modifications to
296 direct chromatin binding and association with interacting partners. Of these modifications,
297 monoubiquitination by the E3 ubiquitin ligase, RAD18, is important for the recruitment of
298 specialized polymerases to bypass obstructive DNA lesions on cellular DNA (16, 38). Our
299 observation that induction of mUb-PCNA is associated with vDNA synthesis (Fig. 1) suggests
300 this is a virus-driven phenomenon. However, the induction of mUb-PCNA may also be a host
301 response to virus infection. For example, increased virus replication is associated with
302 increased oxidative stress (49, 50), and mUb-PCNA induction has been associated with
303 oxidative stress (51, 52). Additionally, induction of mUb-PCNA and its localization to viral RCs
304 could be a response to replication stress that arises due to vDNA synthesis in the nucleus. In
305 this scenario, the association of PCNA with viral genomes might interfere with vDNA synthesis
306 machinery (i.e., pUL54 and pUL44) and ultimately cause a restriction to vDNA synthesis. To
307 further understand the nature and significance of PCNA-K164, future studies should examine
308 the host and or viral proteins that interact with PCNA and regulate post-translational
309 modifications to direct PCNA function during infection.

310 We report that PCNA restricts HCMV-TB40/E replication based on observations that
311 shRNA knockdown of PCNA resulted in increased virus yield (Fig. 2). This was a surprising
312 finding considering that HCMV induces PCNA expression (53, 54) and PCNA localizes to RCs
313 (28, 55) with newly synthesized viral DNA (Fig. 5). Further, PCNA facilitates the replication of
314 other herpesviruses, HSV-1 (35) and EBV (56). For HSV-1, PCNA plays a key role by recruiting
315 viral and cellular factors to sites that facilitate viral genome synthesis (36). Various distinctions
316 between HSV-1 and HCMV, including genome size and differences in the viral processivity
317 factors and kinetics of replication, may underlie how these viruses differentially utilize PCNA.
318 Further, our findings with the low-passage TB40/E strain stand in contrast to previous findings
319 showing that PCNA knockdown decreased HCMV viral genome production in studies using the
320 AD169 strain (30). While we observe that PCNA restricts viral genome synthesis in low MOI

321 infections of TB40/E (Fig. 2C), it is possible that strain differences account for the discrepancy in
322 results. In our study, PCNA knockdown in AD169 infection did not produce a significant change
323 in virus replication (Fig. 2L). AD169 notably lacks 15 kb of viral DNA including many genes
324 important for modulating viral replication for establishment of latency (57). Thus, it is
325 conceivable that some of these genes modulate PCNA in a way that restricts virus replication.
326 For example, pUL145 has been reported to degrade helicase-like transcription factor (HLTF)
327 (58), a multi-functional protein that contains a RING domain which interacts with RAD18 to
328 promote polyubiquitination on PCNA-K164 (40, 59). The strain-dependent differences and the
329 mechanisms by which PCNA restricts HCMV infection remain to be defined.

330 Multiple studies have demonstrated that regulation of PCNA and its post-translational
331 modifications are important for other herpesvirus infections. During infection by the gamma-
332 herpesvirus, Epstein Barr virus (EBV), PCNA is deubiquitinated by the viral enzyme, BPLF1
333 (60). Similarly, PCNA ubiquitination is induced during productive HSV-1 infection and
334 antagonized by the viral deubiquitinating enzyme (DUB), UL36USP (61). Both of these studies
335 showed that deubiquitination of PCNA was important for downregulating pol η recruitment to
336 sites of DNA damage outside the context of infection, but the role of PCNA ubiquitination during
337 viral infection remains to be determined. Notably, Whitehurst et al. show that a PIP domain is
338 conserved among herpesvirus-encoded DUBs, suggesting that these viral enzymes could
339 regulate PCNA. HCMV pUL48 has DUB activity (62); however, a role for pUL48 or host DUBs in
340 deubiquitinating PCNA during infection has yet to be defined. It is possible that herpesvirus
341 infections commonly induce mUb-PCNA but its significance to infection varies among different
342 viruses.

343 PCNA monoubiquitination at K164 is thought to primarily coordinate the DNA damage
344 bypass pathway, TLS. We previously found that TLS polymerases are involved in HCMV
345 infection, whereby Y-family insertion polymerases η , κ , and ι restricted replication, and Rev1 and

346 ζ were required for efficient virus replication (14). Like the insertion TLS polymerases, PCNA
347 restricts HCMV replication, suggesting they could work together through canonical TLS to
348 achieve this effect. Further, similar to previous findings with depletion of TLS polymerases η , κ ,
349 and ι (14), SNVs on vDNA were decreased with depletion of PCNA (Fig. 5C). These
350 observations suggest that PCNA-regulated TLS occurs on the HCMV genome to drive SNVs,
351 consistent with the error-prone nucleotide insertion function of these polymerases (17).
352 Surprisingly, however, PCNA knockdown and rescue with the K164R mutant did not impact SNV
353 counts, suggesting that, while PCNA is important for generation of SNVs, it occurs
354 independently of the mUb-PCNA thought to recruit TLS polymerases to DNA.

355 In contrast to SNVs, PCNA depletion did not increase novel junctions on the genome,
356 indicating no requirement for HCMV genome integrity (Fig. 5A-B), while depletion of TLS
357 polymerases results in increased junctions, primarily inversions (14). Further, rescue of PCNA
358 knockdown with the K164R mutant failed to restore the PCNA-mediated restriction to viral
359 replication (suggesting a requirement for modification at K164, Fig. 3), but had no effect on
360 genome integrity (suggesting the modification on K164 is dispensable for maintaining integrity,
361 Fig. 5). These data suggest that TLS polymerase regulation of HCMV genome integrity occurs
362 independently of PCNA and its monoubiquitination. The fact that depletion of TLS polymerases
363 increased genomic rearrangements, introducing novel junctions on vDNA primarily through
364 sequence inversions, suggests that TLS polymerases are engaging in homology-directed repair,
365 and this occurs independently of PCNA. The function of TLS polymerases in homology-directed
366 recombination are poorly defined (17) and HCMV offers a new tool for defining these roles. For
367 example, $\text{pol}\eta$ and $\text{pol}\kappa$ have been implicated in DNA repair at common fragile sites or difficult-
368 to-replicate regions through a mUb-PCNA-independent mechanism (17, 18). $\text{pol}\eta$ can also
369 function in homology-directed repair pathways, such as break induced replication (BIR), without
370 the involvement of PCNA (19, 20). Intriguingly, the PCNA-independent functions of TLS

371 polymerases are associated with recombination, suggesting that HCMV commandeers Y-family
372 polymerases, but not PCNA, for recombination-dependent repair. This is an intriguing avenue
373 for future studies. However, one possible limitation of these interpretations as they apply to the
374 study is that because we only deplete PCNA levels by 70%, it is possible that the remaining
375 protein is sufficient to permit repair in the presence of TLS polymerases. However, given the
376 phenotypes resulting from the depletion of PCNA on vDNA synthesis, late gene expression,
377 replication and the generation of SNVs, we think this is unlikely.

378 Further, it remains a possibility that in the absence of PCNA, TLS polymerases are
379 recruited by pUL44 or an alternative factor, such as Rev1 (63-65). This would suggest that
380 PCNA and pUL44 compete for interacting partners and provide a possible explanation as to why
381 PCNA restricts HCMV replication. However, our localization studies (Fig. 4), show poor co-
382 localization of PCNA and pUL44 at EdU-labeled replication forks, and PCNA is more closely
383 associated with replication forks than either pUL44 or pUL57. Future studies will address the
384 roles of other factors, such as viral pUL44 or host Rev1, in TLS polymerase repair activity during
385 infection.

386 mUb-PCNA is less closely associated with EdU-labeled replication forks than pUL44 or
387 pUL57, suggesting possible post-synthesis roles that are likely not related to TLS (Fig. 4). The
388 differential subnuclear localization of unmodified and mUb-PCNA implies specific, separable
389 functions of PCNA. It is possible that mUb-PCNA is induced to prevent K164 modification by
390 SUMOylation, which suppresses DNA repair by the homologous recombination pathway (41,
391 42). This would support data in Figure 3 showing that PCNA's suppressive effect on HCMV
392 TB40/E replication is mediated by K164 modification. However, further investigation is required
393 to attribute this to monoubiquitylation, polyubiquitylation, SUMOylation, or a combination of
394 these modifications. Additionally, ubiquitination of PCNA is linked to its retention on chromatin
395 and regulation of nucleosome deposition (66), a function required for HSV-1 infection (35). As

396 PCNA interacts with a wide array of repair proteins, further investigation is required to define
397 mUb-PCNA-associated host and/or viral proteins to elucidate this function.

398 In summary, our findings underscore the intricacy of HCMV interactions with its host,
399 especially with respect to DNA synthesis and repair. Through studying the role of PCNA in
400 HCMV infection, we uncovered multiple, distinct functions of PCNA and, by extension, TLS
401 polymerases on viral genomes that deviate from their canonical function in TLS in host cell
402 biology (Fig. 6). While TLS polymerases engage in canonical TLS repair of vDNA, which is likely
403 PCNA-dependent, but mUb-PCNA-independent, they also likely function in a PCNA-
404 independent manner to protect viral DNA from faulty recombination. Additional work is required
405 to understand specific mechanisms of host machinery-mediated repair of viral genomes by TLS
406 polymerases and the role of PCNA. HCMV infects a large diversity of cell types and has a large,
407 complex exogenous genome, which is readily manipulated. Further, the vDNA is synthesized in
408 the context of cell cycle arrest and inhibition of host DNA synthesis. This allows for the
409 knockdown of critical host factors important to synthesis or repair that would otherwise result in
410 stress or cell death, confounding any results for the requirement in host cell or infection biology.
411 Therefore, HCMV offers an exciting tool to further mechanistically define and separate complex,
412 intermingled DNA synthesis and repair pathways.

413

414 **MATERIALS AND METHODS**

415 **Cells and Viruses.** Primary human lung MRC-5 fibroblasts (ATCC CCL-171) were maintained
416 in DMEM containing 10% FBS as previously described. Cells were infected with the low-
417 passage HCMV strain, TB40/E, a gift from Dr. Christian Sinzger, which was engineered to
418 express green fluorescent protein from the SV40 promoter.

419 **RNAi.** Control shRNA targeting Luciferase was purchased from Sigma-Aldrich (#SHC007). The
420 shRNA targeting PCNA was constructed in the pLKO.1 backbone. In brief, a 21-mer

421 oligonucleotide (GAATGAACCAGTTCAACTAAC) was generated for the target gene and then
422 cloned into pLKO.1 vector via annealing.

423 **Lentivirus and transduction.** Lentiviral particles for shRNA delivery were cultured in HEK 293T
424 cells as previously described. For transduction, MRC-5 fibroblasts were grown to confluence
425 and growth-arrested by contact inhibition to avoid deleterious effects of PCNA depletion in cells
426 undergoing division. Cells were transduced with lentivirus shRNA or rescue constructs at an
427 MOI of 3 in media containing 1 µg/mL polybrene. At two days post transduction, cells were
428 washed in PBS and then given fresh growth media. At four days post transduction, cells were
429 infected with HCMV as described.

430 **Plasmids.** The genetic sequence for human PCNA was amplified from pME-GFP-PCNA
431 (Addgene #105977). Primers containing a sense mutation for shRNA target sequence were
432 used to amplify shRNA-resistant PCNA. Primers containing K164R substitution were used on
433 this sequence to amplify shRNA-resistant PCNA-K164R. PCNA and PCNA-K164R were then
434 expressed from a pCIG vector. All plasmid sequences were validated by Sanger sequencing.

435 **EdU pulse labeling.** Fibroblasts were seeded onto coverslips in 24-well plates in DMEM
436 containing 10% FBS. The next day, cells were washed three times in PBS and growth medium
437 was replaced with serum-free (0% FBS) culture medium. On the following day, cells were
438 infected with HCMV TB40/E at an MOI of 1. At 48 hours post-infection, half of the media was
439 replaced with serum-free DMEM containing 20 µM EdU for a final concentration of 10 µM EdU.
440 Cells were then incubated at 37°C with 5% CO₂. After 10 minutes, the coverslips were washed
441 in PBS and then incubated in cold cytoskeletal (CSK) extraction buffer for two minutes (67).
442 Following CSK extraction, cells were fixed with 100% methanol for 10 minutes at -20°C. After
443 fixation, cells were washed twice with PBS containing 3% BSA. For detection of EdU, the click
444 reaction was performed according to manufacturer instructions (Invitrogen #C10340). Indirect
445 immunofluorescence was subsequently performed as described below.

446 **Immunofluorescence and super-resolution microscopy.** Fibroblasts were seeded onto 12-
447 mm 1.5H high precision coverslips (Marienfeld Superior) in 24-well plates. After EdU pulse
448 labeling (described above), coverslips were processed for indirect immunofluorescence as
449 previously described (14). Briefly, proteins of interest were detected using specific primary
450 antibodies for one hour at room temperature or overnight at 4°C as described in Table 1.
451 Coverslips were washed 3 times in PBS + 0.05% Tween20 and then incubated in secondary
452 antibodies (AlexaFluor 546, AlexaFluor 647, or AlexaFluor 488 goat anti-mouse or goat anti-
453 rabbit [Invitrogen]) for 30 minutes at room temperature. Coverslips were incubated in DAPI for 5
454 minutes and then washed three times in PBS + 0.05% Tween20. Finally, coverslips were
455 mounted onto microscope slides (Fisher Scientific) using Prolong Gold Antifade Mounting
456 Reagent (Invitrogen). Images were obtained using a Zeiss Elyra S.1 super-resolution
457 microscope using a Zeiss 63x Plan-Apochromat 1.40NA objective with structured illumination
458 (SR-SIM) processing. Representative single plane images were adjusted for brightness and
459 contrast using Fiji/ImageJ software.

460 **Colocalization analysis of host and viral proteins to EdU staining in host cell nuclei.**

461 Nikon NIS Elements AR 5.42.03 software with the General Analysis 3 (GA3) module was used
462 for image processing and analysis. The following image processing tools were used to achieve
463 accurate segmentation on the EdU, host protein, and viral protein foci channels: Rolling ball
464 background subtraction (radius = 15px) and Median filter (kernel size = 1px). The Bright Spots
465 Detection tool (diameter = 2px) was used to threshold the EdU, Host, and Viral Protein foci. For
466 DAPI, a Gaussian filter (sigma = 8), rolling ball background subtraction (radius = 220px), and
467 gamma correction (gamma = 0.8) were applied. A Signal Intensity threshold was used to
468 threshold host nuclei and the resulting nuclei binary objects were then modified using Grow
469 Regions and Smooth tools to further refine nuclear segmentation. The AND binary operation
470 was performed between DAPI and corresponding EdU, host protein, and viral protein foci to
471 restrict analysis to only the foci present inside each cell nucleus. To quantify the frequency of

472 colocalization between EdU/Host Foci and EdU/Viral foci, respectively, the AND binary operation
473 was performed between these two paired groups and the Object Count function was used to
474 quantify each group.

475 **Immunoblotting.** Whole cell lysates were extracted using RIPA lysis buffer (Pierce) and manual
476 scraping. 50 µg of lysate was loaded onto precast 4-12% bis-tris gels (ExpressPlus™;
477 GenScript) and then proteins were separated by electrophoresis and transferred onto 0.45 µm
478 pore size PVDF membranes (Immobilon®-FL; Millipore). Proteins of interest were detected
479 using primary antibodies described in Table 1 and fluorophore-conjugated secondary antibodies.
480 Images were obtained using a Li-Cor Odyssey CLx scanner and protein levels were quantitated
481 using Image Studio Lite software.

482 **Genomic sequencing and computational analysis.** Fibroblasts were seeded onto 6-cm
483 dishes and transduced with lentiviral constructs as described above. Five technical replicates
484 were seeded for each condition. At four days post transduction, cells were infected with HCMV-
485 TB40/E at an MOI of 1. Virus inoculum was removed at 2 hpi and cells were provided fresh
486 media. At 96 hpi, when maximal cytopathic effect (CPE) was observed, cells were washed with
487 PBS and collected in DNA lysis buffer containing 200 µg/mL proteinase K by manual scraping.
488 After a two hour 55°C incubation for proteinase K digestion, cellular and viral DNA were isolated
489 using phenol-chloroform extraction. DNA was similarly extracted from the virus stock used for
490 infection. All purified DNA was submitted to SeqCenter (Pittsburgh, PA).

491 Each sample (including virus stocks) was sequenced on a NextSeq 2000 Illumina short
492 read sequencer to yield paired-end short reads. The sequencing reads were aligned to the
493 human reference genome GRCh38 (68) using Bowtie2 v2.5.1 (69) with the following
494 parameters: --very-sensitive for sensitive alignment, --seed 1 for seeding alignment. After
495 alignment, reads aligned to the human genome were filtered out using Samtools v1.17 (70). The
496 following parameters were used: -f UNMAP,MUNMAP to extract reads that were not aligned to
497 the human genome, and -bh to output the filtered alignments in BAM format. HCMV junctions

498 and SNVs were then detected using a two-pass analysis to ensure comparable sequencing
499 coverage between the samples. Non-human reads were first aligned to the reference HCMV
500 genome with breseq v0.38.1 (71) using polymorphism-prediction mode. Using the mean
501 sequencing coverage of reads aligned to the reference from the first breseq run output, the
502 sequencing reads from each sample were subsampled with seqtk v1.4q
503 (<https://github.com/lh3/seqtk>) using parameter -s 100 and the appropriate respective proportions
504 to yield the same mean coverage equal to that of the sample with the lowest coverage (shRNA-
505 Luc). The subsampled FASTQ files were then used to detect the junctions and SNVs by running
506 breseq in the --polymorphism-prediction mode again. Subsequent data analyses were
507 conducted in R version 4.3.2 (72). The novel junctions and SNVs were obtained by removing
508 any of those found in the virus stock samples from the total junctions and SNVs detected in
509 each experimental sample. A Poisson two-sided test was used to compare junction frequency
510 across experimental conditions, with a junction frequency cutoff of 0.025 employed to refine the
511 selection of relevant sequences. Additionally, circle plots were constructed using 'circlize'
512 (version 0.4.16) (73) to visualize the locations and relationships of these sequences, providing a
513 comprehensive view of their distribution and interaction within the genome. This multifaceted
514 approach allowed for a nuanced exploration of genomic junctions, highlighting significant
515 variations and patterns across experimental conditions.

516 **Data availability.** Alignments used for Figure 5 are available at the University of Arizona
517 Research Data Repository (doi: 10.25422/azu.data.27948387). Raw sequence reads have been
518 deposited in the Sequence Read Archive, <https://www.ncbi.nlm.nih.gov/sra> (BioProject ID:
519 SUB14917988).

520 **Table 1. Antibodies used in this study.**

Antibody	Species	Source	Concentration
PCNA	Mouse	Santa Cruz, sc-56	IB 1:1000
PCNA	Rabbit	Cell Signaling Technology (CST), #13110	IF 1:400
mUb-PCNA	Rabbit	CST, #13439	IB 1:1000

			IF 1:100
α -Tubulin	Mouse	Sigma-Aldrich, #T9026	IB 1:2000
IE1/2	Mouse	Thomas Shenk, PhD (Princeton University)	IB 1:100
pUL44	Mouse	Virusys, #CA006	IB, IF 1:12,000
pUL57	Mouse	Virusys, #P1209	IF 1:100
pp150	Mouse	William J. Britt, MD (University of Alabama at Birmingham)	IB 1:15
pp28	Mouse	William J. Britt, MD (University of Alabama at Birmingham)	IB 1:15
Mouse IgG (H+L) secondary, DyLight 680	Goat	Invitrogen, #35519	IB: 1:6000
Rabbit IgG (H+L) secondary, DyLight 800	Goat	Invitrogen, #SA5-10036	IB: 1:6000
Mouse IgG (H+L) secondary, Alexa Fluor 488	Goat	Invitrogen, #A-11029	IF: 1:3000
Rabbit IgG (H+L) secondary, Alexa Fluor 546	Goat	Invitrogen, #A-11035	IF 1:3000
Mouse IgG (H+L) secondary, Alexa Fluor 647	Goat	Invitrogen, #A-21236	IF: 1:3000

521

522

523 **ACKNOWLEDGMENTS**

524 We are grateful to Dr. Jill Dembowski and Dr. Jessica Packard (Duquesne University), Dr.
525 Donald Coen (Harvard University), Dr. Blair Strang (University College of London), Dr. James
526 Alwine (University of Pennsylvania), and Dr. Lynn Enquist (Princeton University) for critical
527 discussion. We acknowledge Emily Jamboretz for technical assistance. The Zeiss Elyra S.1
528 microscope is part of the Imaging Cores – Optical, which is overseen by the University of
529 Arizona’s Office for Research, Innovation, and Impact (purchase of this instrument was
530 supported by NIH S10 OD019948). We acknowledge the assistance of Douglas Crome, MS,
531 Co-Manager of the Imaging Cores – Optical. We are grateful for the support of the Nikon Center
532 of Excellence and the Cancer Center Support Grant P30 CA023074 awarded to University of
533 Arizona. This work was funded by grants from the National Institutes of Allergy and Infectious

534 Diseases to FG (AI079059 and AI079059-14S1) and to FG and GB (AI177392 and AI177392-
535 02S1).

536

537

538 REFERENCES

- 539 1. Goodrum F. 2016. Human Cytomegalovirus Latency: Approaching the Gordian
540 Knot. *Annu Rev Virol* 3:333-357.
- 541 2. Laer Dv, Meyer-Koenig U, Serr A, Finke J, Kanz L, Fauser AA, Neumann-
542 Haefelin D, Brugger W, Hufert FT. 1995. Detection of Cytomegalovirus DNA in
543 CD34+ Cells From Blood and Bone Marrow. *Blood* 86:4086-4090.
- 544 3. Mendelson M, Monard S, Sissons P, Sinclair J. 1996. Detection of endogenous
545 human cytomegalovirus in CD34+ bone marrow progenitors. *Journal of general*
546 *virology* 77:3099-3102.
- 547 4. Boppana SB, Ross SA, Fowler KB. 2013. Congenital Cytomegalovirus Infection:
548 Clinical Outcome: Prenatal Therapy of Congenital Cytomegalovirus Infection.
549 *Clinical infectious diseases* 57.
- 550 5. Cannon MJ. 2009. Congenital cytomegalovirus (CMV) epidemiology and
551 awareness. *J Clin Virol* 46:S6-S10.
- 552 6. Mlera L, Moy M, Maness K, Tran LN, Goodrum FD. 2020. The Role of the Human
553 Cytomegalovirus UL133-UL138 Gene Locus in Latency and Reactivation.
554 *Viruses* 12:714.
- 555 7. Spector DH. 2015. Human cytomegalovirus riding the cell cycle. *Medical*
556 *microbiology and immunology* 204:409-419.
- 557 8. E X, Pickering MT, Debatis M, Castillo J, Lagadinos A, Wang S, Lu S, Kowalik TF.
558 2011. An E2F1-Mediated DNA Damage Response Contributes to the Replication
559 of Human Cytomegalovirus. *PLoS pathogens* 7:e1001342-e1001342.
- 560 9. E X, Kowalik TF. 2014. The DNA Damage Response Induced by Infection with
561 Human Cytomegalovirus and Other Viruses. *Viruses* 6:2155-2185.
- 562 10. Luo MH, Rosenke K, Czornak K, Fortunato EA. 2011. Human Cytomegalovirus
563 Disrupts both Ataxia Telangiectasia Mutated Protein (ATM)- and ATM-Rad3-
564 Related Kinase-Mediated DNA Damage Responses during Lytic Infection (vol 81,
565 pg 1934, 2007). *Journal of virology* 85:3043-3043.
- 566 11. O'Dowd JM, Zavala AG, Brown CJ, Mori T, Fortunato EA. 2012. HCMV-Infected
567 Cells Maintain Efficient Nucleotide Excision Repair of the Viral Genome while
568 Abrogating Repair of the Host Genome. *PLoS pathogens* 8:e1003038-e1003038.
- 569 12. Marians KJ, Kornberg RD. 2018. Lesion Bypass and the Reactivation of Stalled
570 Replication Forks. *Annual review of biochemistry* 87:217-238.
- 571 13. Waters LS, Minesinger BK, Wiltout ME, D'Souza S, Woodruff RV, Walker GC.
572 2009. Eukaryotic Translesion Polymerases and Their Roles and Regulation in
573 DNA Damage Tolerance. *Microbiology and Molecular Biology Reviews* 73:134-
574 154.

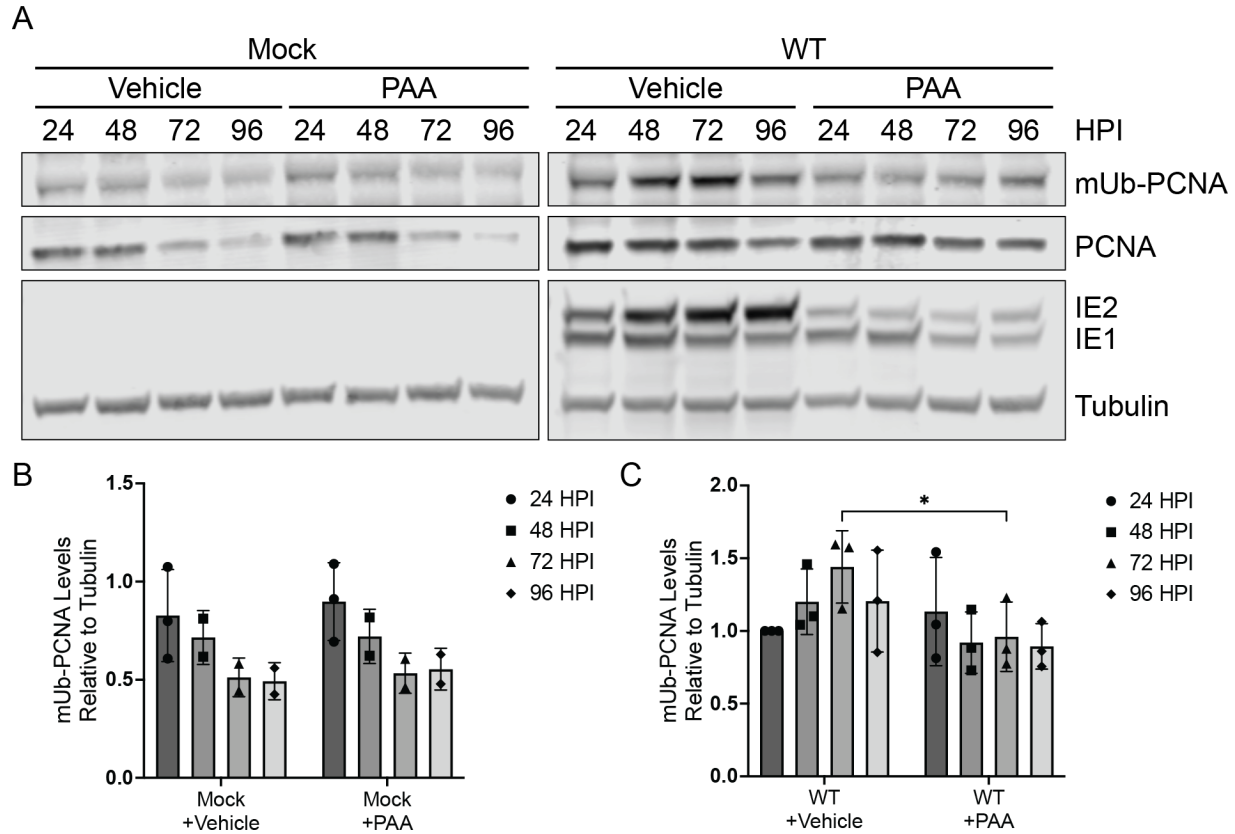
- 575 14. Zeltzer S, Longmire P, Svoboda M, Bosco G, Goodrum F. 2022. Host translesion
576 polymerases are required for viral genome integrity. *Proceedings of the National*
577 *Academy of Sciences - PNAS* 119:e2203203119-e2203203119.
- 578 15. Choe KN, Moldovan G-L. 2017. Forging Ahead through Darkness: PCNA, Still
579 the Principal Conductor at the Replication Fork. *Mol Cell* 65:380-392.
- 580 16. Yang W, Gao Y. 2018. Translesion and Repair DNA Polymerases: Diverse
581 Structure and Mechanism. *Annual review of biochemistry* 87:239-261.
- 582 17. Paniagua I, Jacobs JLL. 2023. Freedom to err: The expanding cellular functions
583 of translesion DNA polymerases. *Molecular cell* 83:3608-3621.
- 584 18. Barnes RP, Hile SE, Lee MY, Eckert KA. 2017. DNA polymerases eta and kappa
585 exchange with the polymerase delta holoenzyme to complete common fragile
586 site synthesis. *DNA repair* 57:1-11.
- 587 19. McIlwraith MJ, Vaisman A, Liu Y, Fanning E, Woodgate R, West SC. 2005.
588 Human DNA Polymerase η Promotes DNA Synthesis from Strand Invasion
589 Intermediates of Homologous Recombination. *Molecular cell* 20:783-792.
- 590 20. Buisson R, Niraj J, Pauty J, Maity R, Zhao W, Coulombe Y, Sung P, Masson J-Y.
591 2014. Breast Cancer Proteins PALB2 and BRCA2 Stimulate Polymerase η in
592 Recombination-Associated DNA Synthesis at Blocked Replication Forks. *Cell*
593 *reports (Cambridge)* 6:553-564.
- 594 21. Zarrouk K, Piret J, Boivin G. 2017. Herpesvirus DNA polymerases: Structures,
595 functions and inhibitors. *Virus research* 234:177-192.
- 596 22. Appleton BA, Brooks J, Loregian A, Filman DJ, Coen DM, Hogle JM. 2006.
597 Crystal structure of the cytomegalovirus DNA polymerase subunit UL44 in
598 complex with the C terminus from the catalytic subunit. Differences in structure
599 and function relative to unliganded UL44. *The Journal of biological chemistry*
600 281:5224-5232.
- 601 23. Ulrich HD. 2009. Regulating post-translational modifications of the eukaryotic
602 replication clamp PCNA. *DNA repair* 8:461-469.
- 603 24. Sinigalia E, Alvisi G, Segré CV, Mercorelli B, Muratore G, Winkler M, Hsiao H-H,
604 Urlaub H, Ripalti A, Chiocca S, Palù G, Loregian A. 2012. The human
605 cytomegalovirus DNA polymerase processivity factor UL44 is modified by SUMO
606 in a DNA-dependent manner. *PloS one* 7:e49630-e49630.
- 607 25. Strang BL, Sinigalia E, Silva LA, Coen DM, Loregian A. 2009. Analysis of the
608 Association of the Human Cytomegalovirus DNA Polymerase Subunit UL44 with
609 the Viral DNA Replication Factor UL84. *Journal of Virology* 83:7581-7589.
- 610 26. Krosky PM, Baek M-C, Jahng WJ, Barrera I, Harvey RJ, Biron KK, Coen DM,
611 Sethna PB. 2003. The Human Cytomegalovirus UL44 Protein Is a Substrate for
612 the UL97 Protein Kinase. *Journal of Virology* 77:7720-7727.
- 613 27. Loregian A, Appleton BA, Hogle JM, Coen DM. 2004. Residues of Human
614 Cytomegalovirus DNA Polymerase Catalytic Subunit UL54 That Are Necessary
615 and Sufficient for Interaction with the Accessory Protein UL44. *Journal of Virology*
616 78:158-167.
- 617 28. Lee SB, Lee CF, Ou DSC, Dulal K, Chang LH, Ma CH, Huang CF, Zhu H, Lin YS,
618 Juan LJ. 2011. Host-viral effects of chromatin assembly factor 1 interaction with
619 HCMV IE2. *Cell research* 21:1230-1247.

- 620 29. Dittmer D, Mocarski ES. 1997. Human cytomegalovirus infection inhibits G1/S
621 transition. *Journal of Virology* 71:1629-1634.
- 622 30. Manska S, Rossetto CC. 2022. Identification of cellular proteins associated with
623 human cytomegalovirus (HCMV) DNA replication suggests novel cellular and
624 viral interactions. *Virology (New York, NY)* 566:26-41.
- 625 31. Huang ES, Huang CH, Huong SM, Selgrade M. 1976. Preferential inhibition of
626 herpes-group viruses by phosphonoacetic acid: effect on virus DNA synthesis
627 and virus-induced DNA polymerase activity. *The Yale journal of biology &*
628 *medicine* 49:93-98.
- 629 32. Lurain NS, Chou S. 2010. Antiviral Drug Resistance of Human Cytomegalovirus.
630 *Clinical Microbiology Reviews* 23:689-712.
- 631 33. Sun Z, Jha HC, Robertson ES. 2015. Bub1 in complex with LANA Recruits PCNA
632 to regulate Kaposi's sarcoma-associated herpesvirus latent replication and DNA
633 translesion synthesis. *Journal of virology* 89:10206-10218.
- 634 34. Daikoku T, Kudoh A, Sugaya Y, Iwahori S, Shirata N, Isomura H, Tsurumi T. 2006.
635 Postreplicative Mismatch Repair Factors Are Recruited to Epstein-Barr Virus
636 Replication Compartments. *The Journal of biological chemistry* 281:11422-11430.
- 637 35. Sanders I, Boyer M, Fraser NW. 2015. Early nucleosome deposition on, and
638 replication of, HSV DNA requires cell factor PCNA. *Journal of neurovirology*
639 21:358-369.
- 640 36. Packard JE, Williams MR, Fromuth DP, Dembowski JA. 2023. Proliferating cell
641 nuclear antigen inhibitors block distinct stages of herpes simplex virus infection.
642 *PLoS pathogens* 19:e1011539-e1011539.
- 643 37. Hoege C, Pfander B, Moldovan G-L, Pyrowolakis G, Jentsch S. 2002. RAD6 -
644 dependent DNA repair is linked to modification of PCNA by ubiquitin and SUMO.
645 *Nature (London)* 419:135-141.
- 646 38. Watanabe K, Tateishi S, Kawasuji M, Tsurimoto T, Inoue H, Yamaizumi M. 2004.
647 Rad18 guides pol η to replication stalling sites through physical interaction and
648 PCNA monoubiquitination. *The EMBO journal* 23:3886-3896.
- 649 39. Xu X, Blackwell S, Lin A, Li F, Qin Z, Xiao W. 2015. Error-free DNA-damage
650 tolerance in *Saccharomyces cerevisiae*. *Mutation research Reviews in mutation*
651 *research* 764:43-50.
- 652 40. Motegi A, Liaw H-J, Lee K-Y, Roest HP, Maas A, Wu X, Moinova H, Markowitz
653 SD, Ding H, Hoeijmakers JHJ, Myung K. 2008. Polyubiquitination of proliferating
654 cell nuclear antigen by HLTF and SHPRH prevents genomic instability from
655 stalled replication forks. *Proceedings of the National Academy of Sciences -*
656 *PNAS* 105:12411-12416.
- 657 41. Moldovan G-L, Dejsuphong D, Petalcorin Mark IR, Hofmann K, Takeda S,
658 Boulton Simon J, D'Andrea Alan D. 2012. Inhibition of Homologous
659 Recombination by the PCNA-Interacting Protein PARI. *Molecular cell* 45:75-86.
- 660 42. Gali H, Juhasz S, Morocz M, Hajdu I, Fatyol K, Szukacsov V, Burkovics P,
661 Haracska L. 2012. Role of SUMO modification of human PCNA at stalled
662 replication fork. *Nucleic acids research* 40:6049-6059.
- 663 43. Ertl PF, Powell KL. 1992. Physical and functional interaction of human
664 cytomegalovirus DNA polymerase and its accessory protein (ICP36) expressed
665 in insect cells. *Journal of Virology* 66:4126-4133.

- 666 44. Weiland KL, Oien NL, Homa F, Wathen MW. 1994. Functional analysis of human
667 cytomegalovirus polymerase accessory protein. *Virus Res* 34:191-206.
- 668 45. Blair LS, Steeve B, Lynne C, David MK, Tomas K, Donald MC. 2012. Human
669 Cytomegalovirus UL44 Concentrates at the Periphery of Replication
670 Compartments, the Site of Viral DNA Synthesis. *J VIROL* 86:2089-2095.
- 671 46. Manska S, Octaviano R, Rossetto CC. 2020. 5-Ethynyl-2'-deoxycytidine and 5-
672 ethynyl-2'-deoxyuridine are differentially incorporated in cells infected with HSV-
673 1, HCMV, and KSHV viruses. *The Journal of biological chemistry* 295:5871-5890.
- 674 47. Schilling E-M, Scherer M, Rothemund F, Stamminger T. 2021. Functional
675 regulation of the structure-specific endonuclease FEN1 by the human
676 cytomegalovirus protein IE1 suggests a role for the re-initiation of stalled viral
677 replication forks. *PLoS pathogens* 17:e1009460-e1009460.
- 678 48. Strang BL, Boulant S, Chang L, Knipe DM, Kirchhausen T, Coen DM. 2012.
679 Human Cytomegalovirus UL44 Concentrates at the Periphery of Replication
680 Compartments, the Site of Viral DNA Synthesis. *Journal of Virology* 86:2089-
681 2095.
- 682 49. Speir E, Shibutani T, Yu Z-X, Ferrans V, Epstein SE. 1996. Role of Reactive
683 Oxygen Intermediates in Cytomegalovirus Gene Expression and in the Response
684 of Human Smooth Muscle Cells to Viral Infection. *Circulation research* 79:1143-
685 1152.
- 686 50. Tilton C, Clippinger AJ, Maguire T, Alwine JC. 2011. Human Cytomegalovirus
687 Induces Multiple Means To Combat Reactive Oxygen Species. *Journal of*
688 *Virology* 85:12585-12593.
- 689 51. Zlatanou A, Despras E, Braz-Petta T, Boubakour-Azzouz I, Pouvelle C, Stewart
690 Grant S, Nakajima S, Yasui A, Ishchenko Alexander A, Kannouche Patricia L.
691 2011. The hMsh2-hMsh6 Complex Acts in Concert with Monoubiquitinated PCNA
692 and Pol η in Response to Oxidative DNA Damage in Human Cells. *Molecular cell*
693 43:649-662.
- 694 52. Kashiwaba S-i, Kanao R, Masuda Y, Kusumoto-Matsuo R, Hanaoka F, Masutani
695 C. 2015. USP7 Is a Suppressor of PCNA Ubiquitination and Oxidative-Stress-
696 Induced Mutagenesis in Human Cells. *Cell reports (Cambridge)* 13:2072-2080.
- 697 53. Zhang X, Tang N, Xi D, Feng Q, Liu Y, Wang L, Tang Y, Zhong H, He F. 2020.
698 Human cytomegalovirus promoting endothelial cell proliferation by targeting
699 regulator of G-protein signaling 5 hypermethylation and downregulation.
700 *Scientific reports* 10:2252-2252.
- 701 54. Song Y-J, Stinski MF. 2002. Effect of the Human Cytomegalovirus IE86 Protein
702 on Expression of E2F-Responsive Genes: A DNA Microarray Analysis.
703 *Proceedings of the National Academy of Sciences - PNAS* 99:2836-2841.
- 704 55. Nitzsche A, Paulus C, Nevels M. 2008. Temporal Dynamics of Cytomegalovirus
705 Chromatin Assembly in Productively Infected Human Cells. *J Virol* 82:11167-
706 11180.
- 707 56. Dyson OF, Pagano JS, Whitehurst CB. 2017. The translesion polymerase pol η is
708 required for efficient epstein-barr virus infectivity and is regulated by the viral
709 deubiquitinating enzyme BPLF1. *Journal of virology* 91.
- 710 57. Wilkinson GWG, Davison AJ, Tomasec P, Fielding CA, Aicheler R, Murrell I,
711 Seirafian S, Wang ECY, Weekes M, Lehner PJ, Wilkie GS, Stanton RJ. 2015.

- 712 Human cytomegalovirus: taking the strain. *Medical Microbiology and Immunology*
713 204:273-284.
- 714 58. Nightingale K, Lin K-M, Ravenhill BJ, Davies C, Nobre L, Fielding CA, Ruckova
715 E, Fletcher-Etherington A, Soday L, Nichols H, Sugrue D, Wang ECY, Moreno P,
716 Umrana Y, Huttlin EL, Antrobus R, Davison AJ, Wilkinson GWG, Stanton RJ,
717 Tomasec P, Weekes MP. 2018. High-Definition Analysis of Host Protein Stability
718 during Human Cytomegalovirus Infection Reveals Antiviral Factors and Viral
719 Evasion Mechanisms. *Cell host & microbe* 24:447-460.e11.
- 720 59. Unk I, Hajdú I, Fátyol K, Hurwitz J, Yoon J-H, Prakash L, Prakash S, Haracska L.
721 2008. Human HLTf functions as a ubiquitin ligase for proliferating cell nuclear
722 antigen polyubiquitination. *Proceedings of the National Academy of Sciences -*
723 *PNAS* 105:3768-3773.
- 724 60. Whitehurst CB, Vaziri C, Shackelford J, Pagano JS. 2012. Epstein-Barr Virus
725 BPLF1 Deubiquitinates PCNA and Attenuates Polymerase η Recruitment to DNA
726 Damage Sites. *Journal of Virology* 86:8097-8106.
- 727 61. Dong X, Guan J, Zheng C, Zheng X. 2017. The herpes simplex virus 1 UL36USP
728 deubiquitinase suppresses DNA repair in host cells via deubiquitination of
729 proliferating cell nuclear antigen. *The Journal of biological chemistry* 292:8472-
730 8483.
- 731 62. Wang J, Loveland AN, Kattenhorn LM, Ploegh HL, Gibson W. 2006. High-
732 Molecular-Weight Protein (pUL48) of Human Cytomegalovirus Is a Competent
733 Deubiquitinating Protease: Mutant Viruses Altered in Its Active-Site Cysteine or
734 Histidine Are Viable. *Journal of Virology* 80:6003-6012.
- 735 63. Weaver TM, Click TH, Khoang TH, Todd Washington M, Agarwal PK, Freudenthal
736 BD. 2022. Mechanism of nucleotide discrimination by the translesion synthesis
737 polymerase Rev1. *Nature communications* 13:2876-2876.
- 738 64. Ohashi E, Murakumo Y, Kanjo N, Akagi Ji, Masutani C, Hanaoka F, Ohmori H.
739 2004. Interaction of hREV1 with three human Y-family DNA polymerases. *Genes*
740 *to cells : devoted to molecular & cellular mechanisms* 9:523-531.
- 741 65. Guo C, Sonoda E, Tang T-S, Parker JL, Bielen AB, Takeda S, Ulrich HD,
742 Friedberg EC. 2006. REV1 Protein Interacts with PCNA: Significance of the
743 REV1 BRCT Domain In Vitro and In Vivo. *Molecular cell* 23:265-271.
- 744 66. Thakar T, Leung W, Nicolae CM, Clements KE, Shen B, Bielinsky AK, Moldovan
745 GL. 2020. Ubiquitinated-PCNA protects replication forks from DNA2-mediated
746 degradation by regulating Okazaki fragment maturation and chromatin assembly.
747 *Nature communications* 11:2147-14.
- 748 67. Dimitrova DS, Gilbert DM. 2000. Stability and Nuclear Distribution of Mammalian
749 Replication Protein A Heterotrimeric Complex. *Experimental cell research*
750 254:321-327.
- 751 68. Schneider VA, Graves-Lindsay T, Howe K, Bouk N, Chen H-C, Kitts PA, Murphy
752 TD, Pruitt KD, Thibaud-Nissen F, Albracht D, Fulton RS, Kremitzki M, Magrini V,
753 Markovic C, McGrath S, Steinberg KM, Auger K, Chow W, Collins J, Harden G,
754 Hubbard T, Pelan S, Simpson JT, Threadgold G, Torrance J, Wood JM, Clarke L,
755 Koren S, Boitano M, Peluso P, Li H, Chin C-S, Phillippy AM, Durbin R, Wilson
756 RK, Flicek P, Eichler EE, Church DM. 2017. Evaluation of GRCh38 and de novo

- 757 haploid genome assemblies demonstrates the enduring quality of the reference
758 assembly. *Genome research* 27:849-864.
- 759 69. Langmead B, Salzberg SL. 2012. Fast gapped-read alignment with Bowtie 2.
760 *Nature methods* 9:357-359.
- 761 70. Li H, Handsaker B, Wysoker A, Fennell T, Ruan J, Homer N, Marth G, Abecasis
762 G, Durbin R. 2009. The Sequence Alignment/Map format and SAMtools.
763 *Bioinformatics* 25:2078-2079.
- 764 71. Deatherage DE, Barrick JE. 2014. Identification of Mutations in Laboratory-
765 Evolved Microbes from Next-Generation Sequencing Data Using breseq. 165-
766 188.
- 767 72. Team RC. 2023. R: A Language and Environment for Statistical Computing. R
768 Foundation for Statistical Computing, Vienna, Austria.
- 769 73. Gu Z, Gu L, Eils R, Schlesner M, Brors B. 2014. circlize Implements and
770 enhances circular visualization in R. *Bioinformatics (Oxford, England)* 30:2811-
771 2812.
- 772
- 773
- 774



775

776 **Figure 1. mUb-PCNA increases with viral DNA synthesis.**

777 Fibroblasts were mock-infected or infected (MOI = 1) with TB40/E-WT virus over a 96-hour time

778 course. Immunoblotting was performed on whole cell lysates collected at the indicated time

779 points. (A) mUb-PCNA and PCNA were detected using monoclonal antibodies specific to each

780 and secondary antibodies conjugated to DyLight™ 680 (mouse) or 800 (rabbit). IE1/2 are

781 immediate early proteins that serve as a marker for progression of virus replication. Tubulin

782 serves as a loading control. mUb-PCNA levels relative to tubulin were quantified in (B) mock-

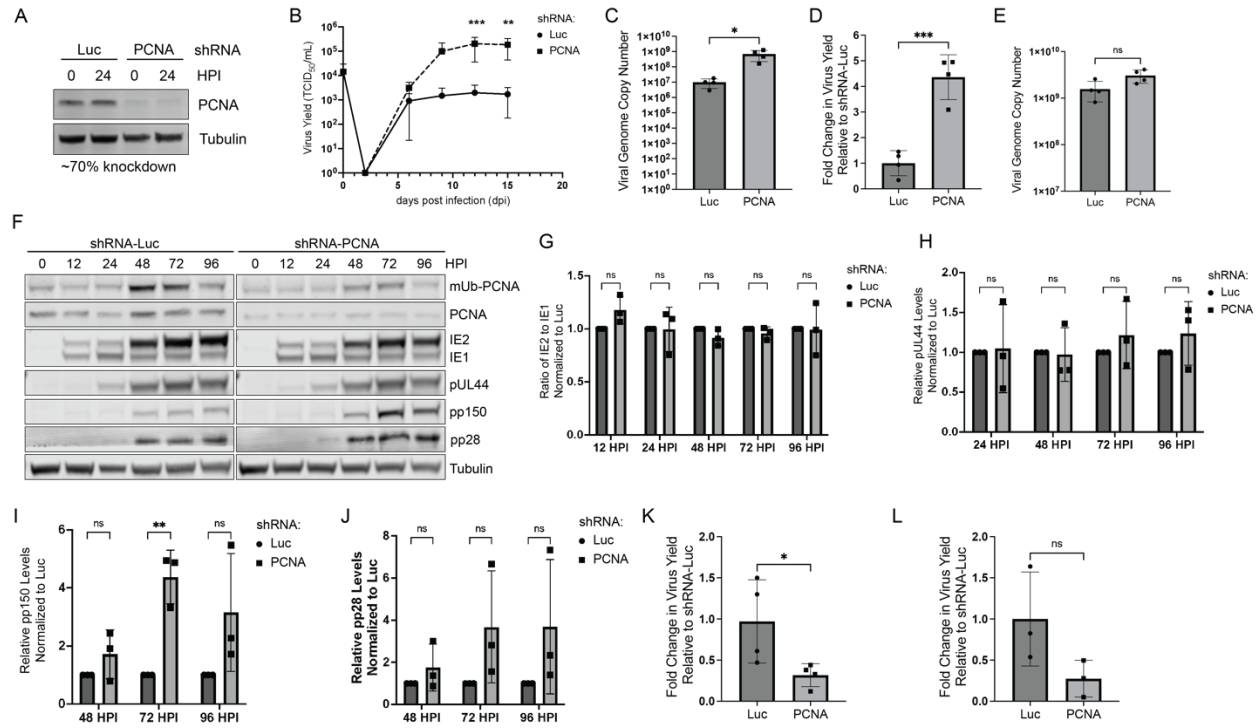
783 infected and (C) TB40/E-infected conditions and normalized to the 24 hpi time point.

784 Statistical analysis was performed by two-way ANOVA with Tukey's multiple comparisons test.

785 Asterisks (*P <0.05) represent statistically significant differences determined in three

786 independent experiments.

787



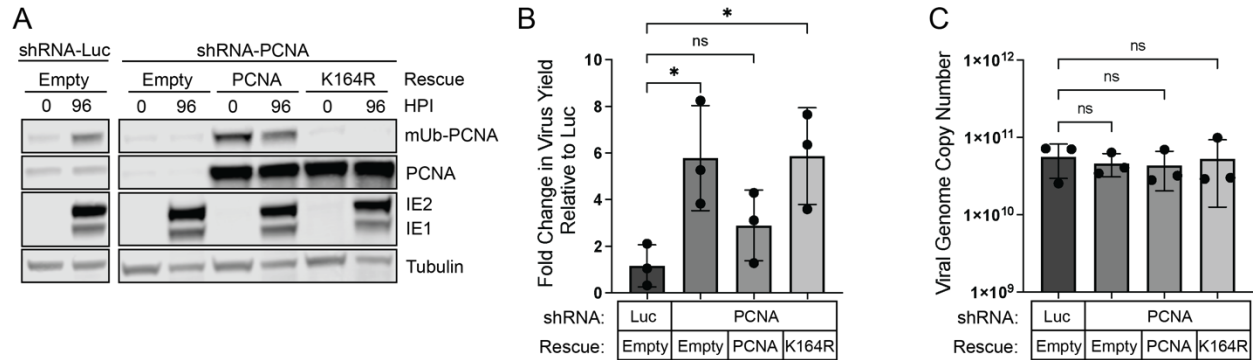
788

789 **Figure 2. PCNA restricts HCMV TB40/E replication.**

790 (A-C) Growth-arrested fibroblasts expressing shRNA against PCNA or Luciferase (Luc, non-
 791 targeting control) were infected with TB40/E-WT at an MOI of 0.02. (A) Whole cell lysates were
 792 collected at the time of infection (0 hpi) and at 24 hpi and then immunoblotted. To confirm
 793 knockdown, PCNA was detected using a monoclonal antibody. An average knockdown of 70%
 794 was achieved over multiple independent experiments. (B) Virus yield at 15 dpi were determined
 795 by TCID₅₀ and normalized relative to the Luc control. (C) Viral genome copy number at 15 dpi
 796 was determined by qPCR using a TB40/E BAC standard curve and primer set designed for the
 797 region of the viral genome encoding the β 2.7 transcript. (D-F) Growth-arrested fibroblasts
 798 expressing shRNA against PCNA or Luc were infected with TB40/E-WT at an MOI of 1. (D)
 799 Virus yield at 96 hpi was determined by TCID₅₀ and normalized relative to the Luc control. (E)
 800 Absolute viral genome copy number was determined by qPCR using a standard curve. (F)
 801 Whole cell lysates were collected over a 96 hour time course (0 hpi = time of infection) and
 802 immunoblotted. To confirm knockdown, PCNA and mUb-PCNA were detected using monoclonal

803 antibodies to each. The following proteins were also detected as markers for the viral gene
804 expression cascade: IE1/2 (immediate early), pUL44 (early), pp150 and pp28 (late) with
805 secondary antibodies conjugated to DyLight™ 680 (mouse) or 800 (rabbit). Tubulin serves as a
806 loading control. (G-J) Quantification of immunoblots in *F* for (G) IE1/2, (H) pUL44, (I) pp150 and
807 (J) pp28 with PCNA knockdown normalized to Luc for each time point. (K) Growth-arrested
808 fibroblasts expressing shRNAs were infected with HSV-1 at an MOI of 0.01 and virus yields
809 were determined relative to the Luc control at 33 hpi. (L) Growth-arrested fibroblasts expressing
810 shRNAs were infected with HCMV AD169-GFP (WT) at an MOI of 1, and virus yield was
811 determined relative to the Luc condition at 96 hpi. For statistical analysis, significance was
812 determined by two-way ANOVA with Tukey's multiple comparisons test (B), two-way ANOVA
813 with Sidak's multiple comparisons test (G-J) or an unpaired t test (C-E, K-L). Asterisks (*P
814 <0.05, **P <0.01, ***P <0.001) represent statistically significant differences determined in a
815 minimum of three independent experiments.
816

817



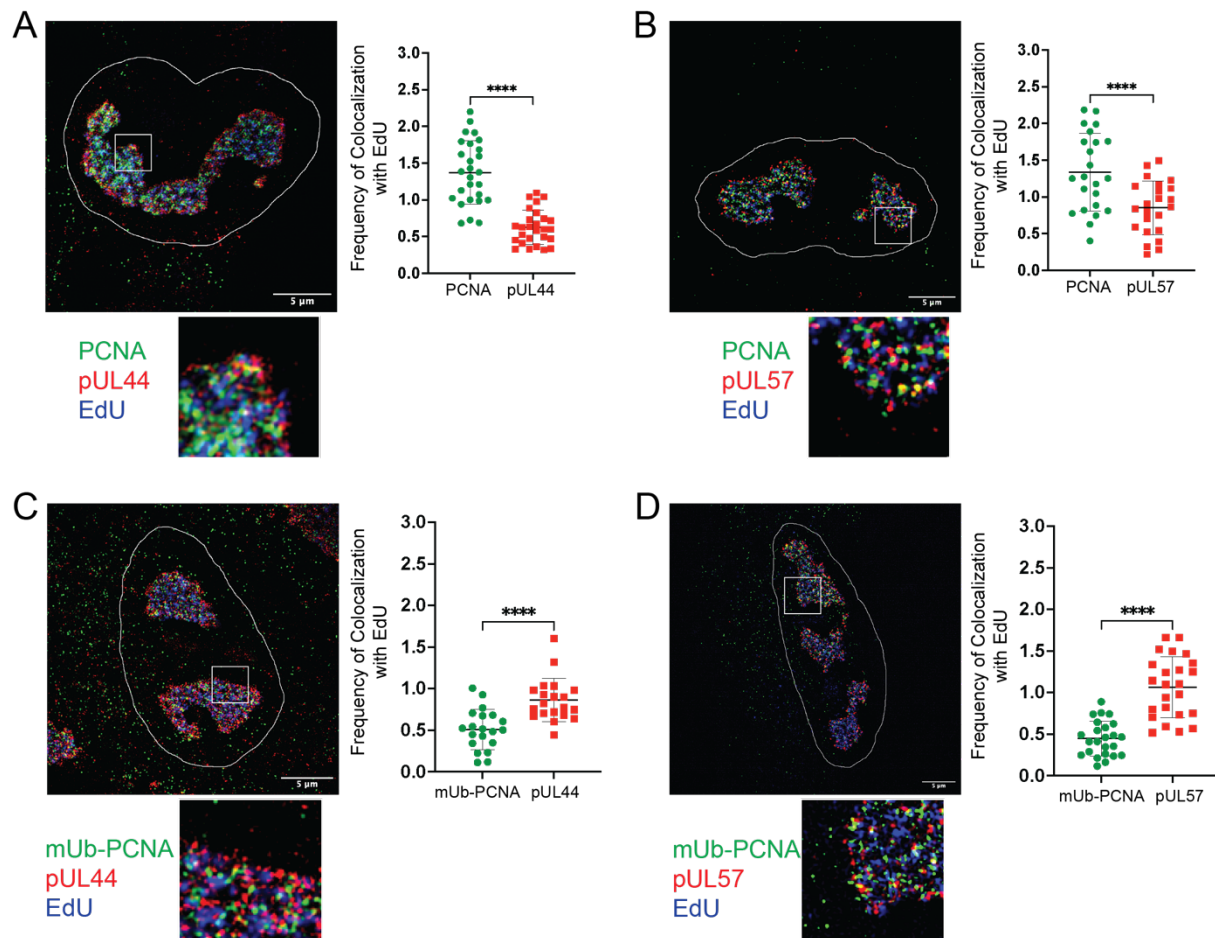
818

819 **Figure 3. PCNA K164 modification mediates restriction of HCMV replication.**

820 Growth-arrested fibroblasts were transduced with lentiviral particles expressing shRNAs
 821 (targeting PCNA or Luciferase). Simultaneously, cells were transduced to overexpress shRNA-
 822 resistant PCNA (wild-type or mutant containing a lysine-to-arginine mutation at amino acid 164
 823 [K164R]) or an empty overexpression vector control. Cells were infected with HCMV at an MOI
 824 of 1 at 48 hours post transduction and collected at 96 hpi. (A) To confirm protein knockdown and
 825 rescue, whole cell lysates were collected at the time of infection (0 hpi) or at 96 hpi. mUb-PCNA,
 826 PCNA, tubulin, and IE1/2 were detected using monoclonal antibodies as shown with secondary
 827 antibodies conjugated to DyLight™ 680 (mouse) or 800 (rabbit). (B) Virus yields were measured
 828 by TCID50 and normalized relative to Luc. (C) Viral genome copy number was determined by
 829 qPCR using a TB40/E BAC standard curve and primer set designed for the region of the viral
 830 genome encoding the b2.7 transcript. Statistical significance was determined by one-way
 831 ANOVA with Tukey's multiple comparisons test. Asterisks (**P <0.01) represent statistically
 832 significant differences determined in independent experiments.

833

834



835

836

837

838 **Figure 4. mUb-PCNA localizes to distinct replication compartment subdomains.**

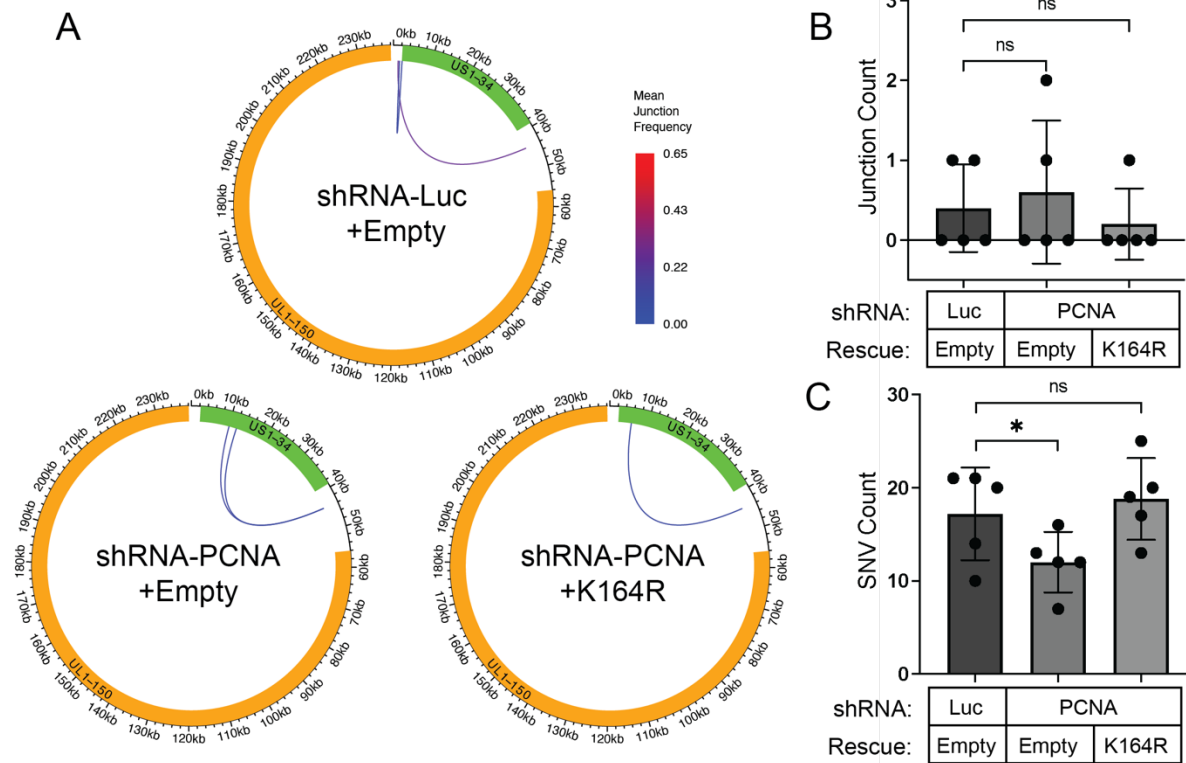
839 Fibroblasts were serum-starved and then infected with TB40/E-WT at an MOI of 1. At 48 hpi,
840 cells were pulsed with 10 μ M EdU for 10 minutes, CSK-extracted, and fixed. All coverslips were
841 washed and then a click reaction was performed to conjugate EdU and Alexa Fluor 647 (blue)
842 for detection. Indirect immunofluorescence was then carried out using monoclonal antibodies to
843 the indicated proteins: (A) PCNA and pUL44, (B) PCNA and pUL57, (C) mUb-PCNA and pUL44,
844 (D) mUb-PCNA and pUL57 with secondary antibodies conjugated to Alexa Fluor® 546 (green)
845 or 488 (red). DAPI-stained nuclei (not pictured) were outlined using Fiji/ImageJ software. An

846 enlargement of the boxed area is shown below each image. Images were captured using a
847 Zeiss Elyra S.1 super-resolution microscope. Scale bar, 5 μm . The frequency of colocalization
848 between host or viral proteins and EdU was quantified using Nikon NIS Elements software (see
849 Materials and Methods) and is shown to the right of each image with each point representing a
850 cell. Statistical significance was determined by a paired t test. Asterisks (****P <0.0001)
851 represent statistically significant differences determined in three independent experiments.

852

853

854

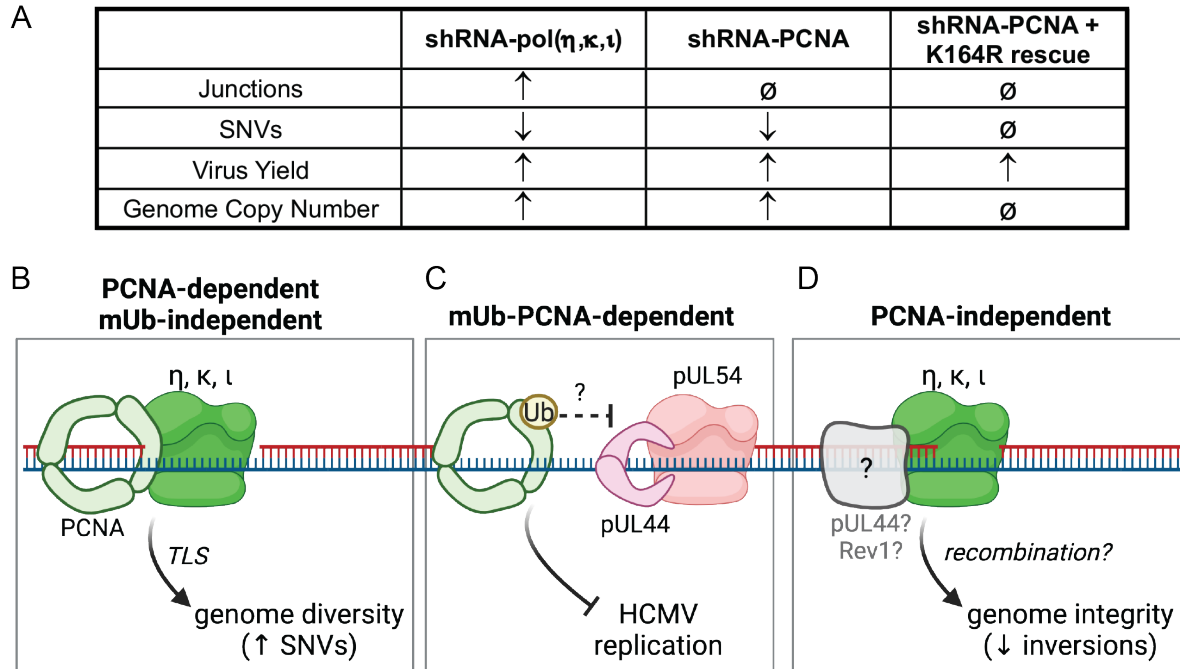


855

856 **Figure 5. PCNA contributes to HCMV genome diversity but not integrity.**

857 Growth-arrested fibroblasts were transduced with lentiviral particles expressing shRNAs against
 858 PCNA or Luciferase at an MOI of 3. Simultaneously, cells were transduced to overexpress
 859 shRNA-resistant PCNA-K164R or an empty overexpression vector control. Forty-eight hours
 860 later, media was refreshed with puromycin at 2 $\mu\text{g}/\text{mL}$; 24 hours later, cells were infected with
 861 TB40/E-WT at an MOI of 1 and total DNA was isolated at 96 hpi for sequencing. Sequences
 862 from each knockdown condition as well as from the virus stock used for infection were aligned
 863 to the TB40/E-GFP reference genome. (A) Mean novel junction frequency within each condition.
 864 HCMV genomic coordinates are plotted along the circular axis in graphs for each condition and
 865 the UL (orange) and US (green) regions of the genome are marked. The arcs connect novel
 866 junction points detected at the average frequency for the given condition indicated by the color
 867 scale. (B) Quantification of the number of novel junctions (inversions, deletions, duplications)
 868 detected per sample ($n = 5$) for each condition. (C) Quantification of the number of novel SNVs

869 (point mutations, deletions, or insertions) detected per sample ($n = 5$) for each condition.
870 Statistical significance was determined by pairwise two-sided exact Poisson tests and adjusted
871 using Bonferroni correction. Asterisks ($*P < 0.05$) represent statistically significant differences
872 determined in independent experiments.
873



874

875 **Figure 6. Model for the varied roles of PCNA and TLS polymerases in HCMV DNA**

876 **synthesis and genome integrity.** (A) Summary of observed virus infection phenotypes with

877 host factor knockdown. Table depicts an observed increase (↑), decrease (↓), or no change (∅)

878 for each unique condition relative to control (shRNA-Luc). (B) PCNA and TLS polymerases are

879 required for viral genome diversity. In a mUb-PCNA-independent manner, PCNA and error-

880 prone Y-family TLS polymerases η , κ , and ι , engage in TLS repair on vDNA, contributing to

881 generation of SNVs and genome diversity. (C) PCNA restricts HCMV replication dependent on

882 its modification at K164. While an exact mechanism remains to be defined, PCNA could

883 compete with or inhibit functions of the viral processivity factor, pUL44, and DNA polymerase,

884 pUL54. (D) TLS polymerases have PCNA-independent functions in HCMV genome integrity. Y-

885 family TLS polymerases η , κ , and ι maintain HCMV genome integrity by preventing inversions

886 on vDNA, likely through recombination-dependent repair. This repair is independent of PCNA

887 and possibly involves an alternative factor, such as pUL44 or Rev1.

888